Journal of the Korean Physical Society, Vol. 50, No. 5, May 2007, pp. 1271∼1275

Energy Shift During Ion Extraction from an ICP Source

O. V. Vozniy*
Department of Materials Engineering, Sungkyunkwan University, Suwon 440-746 and Kharkiv Scientific Center of Physics and Technologies, Kharkiv, Ukraine

B. J. Park, K. S. Min and G. Y. Yeom
Department of Materials Engineering, Sungkyunkwan University, Suwon 440-746

(Received 18 December 2006, in final form 16 March 2007)

In this work, the deviation of energy distribution function of energetic ions from the predetermined value in an inductively coupled plasma (ICP) ion gun source is discussed. An abnormal plasma potential increase at an extraction voltage 400 V caused a beam energy shift of up to 50 eV compared to the preset value. The ion energy peak position was found to be more affected by pressure at higher extraction voltages on the acceleration grid. The energy of primary and secondary ions was measured with an ion energy analyzer. The evolution of the ion energy distribution function during the accelerating voltage change was studied in the pressure range from 3×10^{-3} to 1.1×10^{-2} Torr.

PACS numbers: 52.40.Hf, 52.40.Mj
Keywords: Inductively coupled plasma, Sheath, Ion energy distribution function

I. INTRODUCTION

At present time, mostly due to development of a technique for precise surface etching and for producing nanometer size structures, an inductively coupled plasma (ICP) is widely used as a common instrument for technological processing [1–4]. ICP sources are capable of generating ion beams of low energy and high flux. On the one hand, the ion energy is not sufficient to change the bulk characteristics of the sample; on the other, due to the low energy spread of the incident particles, the required level of selectivity can be achieved during the etching of surfaces that are partially covered with photoresist [5]. In contrast to others sources utilizing ion optics, a three-grid system allows one to obtain highly focused ion beams with defined energies. In spite of the high ion densities of the generated beams, the ICP source makes possible uniform etching of homogeneous materials over the entire area of the processed surface.

One of the most important parameters characterizing any plasma source is the ion energy distribution function (IEDF). In an ICP, it shows strong dependence on the pressure, the magnitude of plasma potential, and the length of the sheath that is formed not only on the dielectric chamber walls but also at regions adjacent to the acceleration electrodes. As was shown in Ref. 6, the dependence of the distribution function on the pressure becomes significant when the amplitude of oscillation of the ion in an electromagnetic field becomes comparable with the sheath length.

At the present time, in connection with the necessity to receive structures whose typical sizes do not exceed several nanometers, the methods of beam formation should be studied to receive ion fluxes with strongly defined energies. That is why in analyzing such a source one should consider not only the characteristics of the ion optics but also the number of plasma processes determining the additional energy of the ions leaving the discharge volume. This additional energy may reach 10 % of the beam energy in absolute value, which can lead to overetching of the sample. Besides, the higher the plasma potential at a given acceleration voltage, the higher the energy spread of the ion distribution function, which decreases the etching selectivity.

In spite of the fact that the electromagnetic field in the antenna, in the dielectric wall and in the electrically neutral plasma is a sinusoidal function, inside the sheath it is not harmonic. As a result, the plasma acquires a positive potential relative to the walls of the discharge chamber. When no voltage is applied to the acceleration grid, the ion energy is determined by the magnitude V_{0p}, which is part of the equation for the plasma potential $V_p = V_{0p} + V_a \sin(\omega t)$ (in case of a purely inductive coupling, the alternating component can be neglected). V_{0p} equals to the average value of the potential difference between the plasma and the initially floating electrode over the period of a plasma oscillation. The magnitude V_a is obviously smaller than V_{0p}, owing to the limited velocity

*E-mail: oleksiy@skku.edu

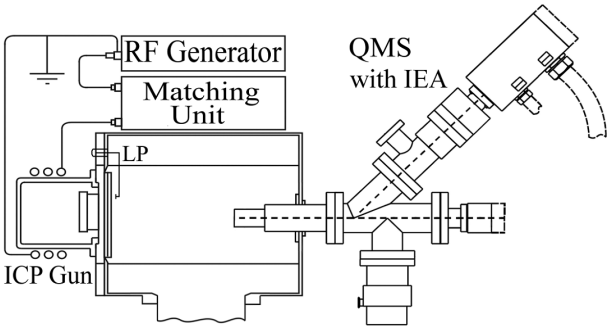

Fig. 1. Schematic view of the 13.56-MHz ICP ion beam source with a set of diagnostic tools, including a QMS with an ion energy analyzer.

of the charge carriers in the RF oscillating field. The authors of the work [7] demonstrated that eV_{0p} equals the beam energy within an accuracy of $3-5$ eV. Thus, the additional beam energy that is observed during ion extraction by means of the grid electrode system is determined by the magnitude $e(V_{0p}-V_{1g})$, where V_{1g} is the first grid voltage.

In a three-grid ion optical system, the position of the plasma boundary is controlled by the potential difference between the first and the second electrodes [8]. The boundary also can move at a constant extraction voltage when the pressure is increased due to continuity between the Child-Langmuir current and the Bohm current. This process is accompanied by a plasma potential decrease.

The additional ion energy also depends on the number of ion collisions and on the number of oscillating cycles in the RF field [6] during the time when it travels through the sheath. However, in this paper, we consider only influence of the magnitude V_p-V_{1g}, as well as the pressure inside the discharge volume, on additional beam energy,.

II. EXPERIMENT

Figure 1 illustrates a schematic diagram of the experimental setup. A detailed description of the ICP reactor can be found elsewhere [9]. The plasma was generated by means of electromagnetic oscillations with a nominal frequency of 13.56 MHz inside a spiral-type antenna. The RF generator load resistance was tuned by using a π-type matching unit. Ion beam formation and focusing were provided by a system of accelerating electrodes. The ion optics of the source included planar grids, which were mounted 2 mm apart. The screen grid, the decelerator, and the accelerator grids, 96 mm in diameter with a thickness of 1 mm, contained 2.0-mm holes in a 3.0-mm hexagonal raster. Other grid geometries and materials were tested and are available.

The ion energy was measured by using an ion energy analyzer integrated into a quadrapole mass-spectrometer (QMS) (Hiden Analytical). The distance between the ion source and the analyzer inlet was equal 25 cm. The IEDF was less affected by collisions at the beam transportation area due to the strong pressure gradient between the gun and the analyzer inlet. An investigation of a given source type is necessary for a correct description of etching systems that are capable to generating beams of neutral molecules or radicals [10,11] to avoid charge-induced damage during the plasma treatment [12]. The given method of ion additional energy determination is not disturbing, in contrast to methods employing emissive probes [13].

The pressure in the chamber was controlled by using a Granville-Phillips ion gauge, Model 274006, located between the source and the QMS inlet. A planar Langmuir probe was installed to measure the ion current inside and outside the ion source.

III. RESULT AND DISCUSSION

IEDF profile analysis provides information on sheath and pre-sheath characteristics, such as the potential drop near the chamber walls and the energy transfer mechanisms, including inelastic collisions and charge exchange [14, 15]. The plasma potential is always higher than the first electrode voltage due to high electron mobility. Therefore, electroneutrality near the electrode is not preserved at the region where the electrons experience strong deceleration in a repulsive field, *i.e.*, at the outer boundary of the space charge distribution, where a negative potential relatively undisturbed plasma is close to the magnitude kT_e/e. For quasi-neutrality maintenance, the ions coexist with more energetic electrons at the sheath boundary. Thus the ion density in this region approximately equals the electron density, *i.e.*, is close to $n_0\exp(-e|V^*|/kT)$, where V^* is the potential relative to V_p. In the case of low pressure and electron Maxwellian distribution, the plasma potential can be found from the expression for the current collected by a Langmuir probe installed inside the ICP source:

$$j_i = en_e\Big(\frac{kT_e}{2\pi m_i}\Big)^{1/2}\exp\Big(-\frac{e}{kT_e}|V_p-V_{1g}|\Big), \qquad (1)$$

where V_{1g} is the grid potential, n_e and T_e are the electron density and temperature respectively, and m_i is the ion mass.

For pressures higher than 10^{-2} Torr, the form of the IEDF is determined not only by the plasma potential but also by the number of ion cycles in the RF field during the ion's travel through the sheath, as well as by collisions taking place there. Collisions then often result in a smoothing of the distribution function and give rise to additional IEDF peaks due to modifications of the sheath structure and of the charge distribution in it. Since there are no energetic electrons in the sheath [16], inelastic collisions of ions with neutral gas atoms play an essential

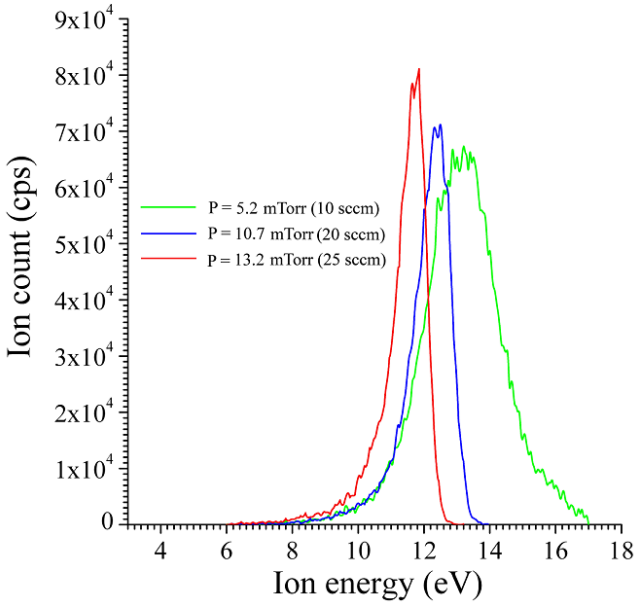

Fig. 2. IEDs of an Ar^+ ion beam for different pressures without voltage on the acceleration grid. The output power is $P = 200$ W.

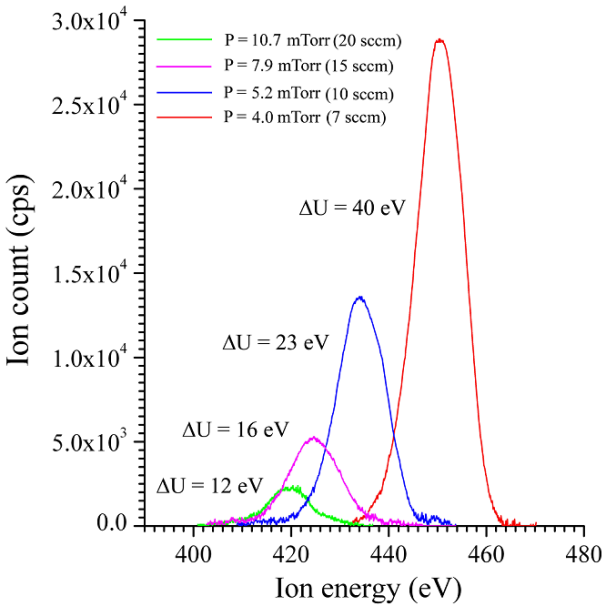

Fig. 3. IEDs of Ar+ ions for 4×10^{-3} (the highest peak), 5.2×10^{-3}, 7.9×10^{-3} and 1.07×10^{-2} Torr. The accelerating voltage is 410 V, and the output power is $P = 200$ W.

role in the formation of the IEDF and, correspondingly, in establishing the plasma potential. The number of inelastic collisions is determined by the formula

$$\nu_i(T_i) = n_n K(T_i) = \frac{8\pi n_n}{\sqrt{m_i}}\Big(\frac{1}{2\pi e T_i}\Big)^{3/2} \times \int_0^\infty \sigma(E_i) E_i \exp\Big(\frac{-E_i}{eT_i}\Big) dE_i, \quad (2)$$

where $K(T_i)$ is the collision rate constant, n_n is the neutral gas density, E_i is the ion energy, and σ is the collision cross-section [17].

When the ions travel through a positive space charge sheath, the current on the grid electrode is determined by the Bohm criterion. The relation between the plasma and the 1^{st} grid potential is given by the equation

$$V_p - V_{1g} = T_e \ln\Big(\frac{m_i}{2\pi m_e}\Big)^{1/2}. \quad (3)$$

T_e is the electron temperature, and m_e and m_i are the electron and the ion mass respectively.

The variation of the plasma potential at the floating electrode doesn't exceed $2 - 3$ V in the pressure range $5 \times 10^{-3} - 1.3 \times 10^{-2}$ Torr as follows from IEDF measurements shown in Figure 2 in the case when no potential was applied to the acceleration grids. The increase in the plasma potential with decreasing operating pressure is a well known phenomenon, because the lower rate of inelastic collisions of electrons with atoms causes the electron temperature to increase so that more electrons escape to the wall and the potential of bulk plasma increases [18]. As we see from Figure 2, the influence of the pressure on the plasma potential near the floating electrode is not critical. However, the plasma potential increases drastically compared to the voltage of the first grid during extraction of high energy ions. Figure 3 shows the IEDF of energetic ions when the first grid potential is 410 V for pressures of 4.0×10^{-3}, 5.2×10^{-3}, 7.9×10^{-3}, and 1.1×10^{-2} Torr. The energy is denoted with ΔU, which is gained by the ions during their travel through the potential difference at the sheath. The expected value of the beam energy was 410 eV or a few eV larger, but as is seen from the picture, the difference between the preset magnitude of the ion energy and its real value determined by the plasma potential can reach 40 eV at lower pressures.

There are at least two effects determining the magnitude of the plasma potential. First, as was mentioned before, ion inelastic collisions with neutrals can significantly change the sheath structure, in particular the thickness and the position relative to the grid holes. Second, the transition region between the bulk plasma and the space where the ions are accelerated in the electrical field of the grid system is not stationary when the pressure is changed. At that, if the ion current in the plasma is limited by the Bohm criterion,

$$j_b \cong 0.6 e n_e \Big(\frac{kT_e}{m_i}\Big)^{1/2}, \quad (4)$$

then outside, it is determined by the Child-Langmuir equation

$$j_i = \frac{4\varepsilon}{9}\Big(\frac{2e}{m_i}\Big)^{1/2}\frac{V_0^{3/2}}{h^2}. \quad (5)$$

Here, m_i is the ion mass, $V_0 = V_p - V_{1g}$, and h is the

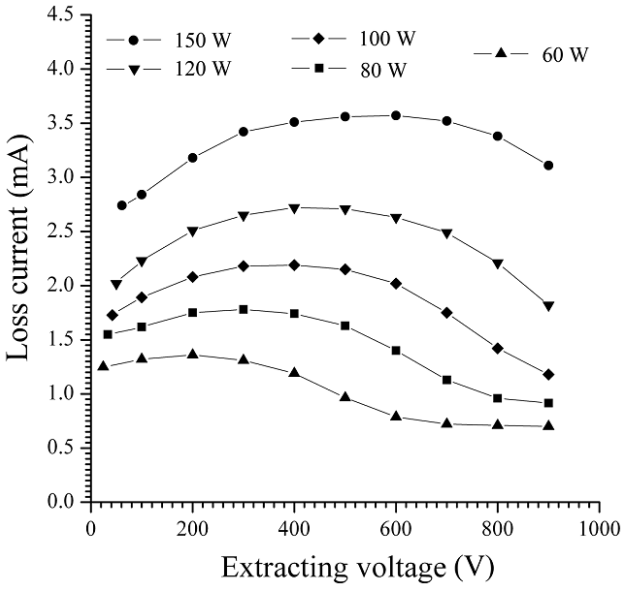

Fig. 4. Loss current due to plasma boundary movement during extraction voltage increase.

sheath length. Due to the continuity of the electrical current, the condition $j_b = j_i$ should be fulfilled. If the ion flux exceeds the vacuum current limit ($j_b > j_i$), for example during a pressure increase, then the plasma expands to reduce the gap h between the bulk plasma and the electrode until a flux balance is achieved. Since the current j_i depends on the plasma potential, there is a certain correlation between it and the plasma boundary position.

Figure 3 also presents the ion current loss at higher pressures, which is caused by a plasma potential decrease. At this plasma surface, limited by the sheath, changes its curvature near the extraction holes, which leads to beam defocusing and a higher rate of ion loss on the second grid. To prove that the plasma surface deformation takes place for different plasma potentials, we measured the dependence of the loss current on the magnitude of extraction voltage between the first and the second grids (Figure 4). The second grid was under a constant negative potential whereas the voltage of the first one was varied from 0 to 900 V. This procedure changes the magnitude of the loss current due to the plasma boundary movement and, consequently, due to the plasma potential variation [8]. It is logical to assume that the beam intensity decrease (Figure 3) during a pressure increase at a constant acceleration voltage would also be accompanied by a plasma boundary movement.

In the general case, the integral current density increases linearly when the pressure grows [19], as it is evidenced by the Langmuir probe measurements inside the source shown in Fig 5. At a pressure of 5.5×10^{-3} Torr the slope of the curve becomes smaller. This is due to Eq. (5) losing applicability, due to inelastic collisions,

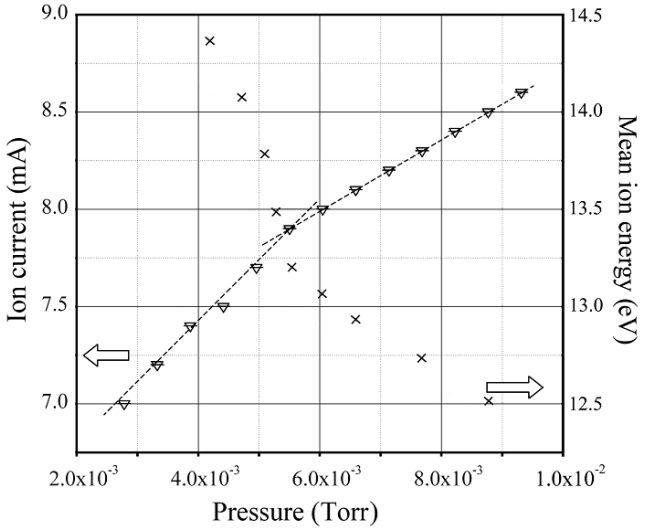

Fig. 5. Ion current inside an ICP near the grid electrode and the mean Ar^+ ion energy as functions of pressure.

as the pressure approaches 10^{-2} Torr. Eq. (6) should be used instead of Eq. (5) in the transition pressure range [20]:

$$V_0 = \frac{6h^{4/3}}{5} \cdot \left(\frac{m_i}{2e} \cdot \frac{h+\lambda_i}{\lambda_i}\right)^{1/3} \cdot \left(\frac{h+\lambda_i}{2h+\lambda_i}\right) \cdot (6\pi j_i)^{2/3}, \tag{6}$$

where V_0 is the time-average plasma potential relative to the first electrode, λ_i is the ion mean free path in the neutral gas environment, and h is the sheath length.

It follows from Eq. (6) that the plasma potential $V_p = V_0 - V_{1g}$ increases when the ion mean free path λ_i in a neutral gas becomes smaller. At the same time, the plasma potential is affected by the pressure due to a perturbation in the balance of the continuity law $j_i = j_b$ because Eq. (4) for the Bohm current includes the electron density and temperature in the plasma. Both magnitudes significantly depend on the number of inelastic collisions of ions with electrons and atoms of residual gas.

Figure 5 illustrates the evolution of the Ar ions mean energy, which is determined by Eq. (7), as a function of pressure:

$$\langle E_i \rangle = \frac{\int_0^\infty EF(E)dE}{\int_0^\infty F(E)dE}, \tag{7}$$

where $F(E)$ is the ion distribution function. The dependence also has two regions with different slopes, as it was for the ion current, indicating that the ion's mean energy, determined by the plasma potential, and the current intensity are interdependent parameters. Beginning from a pressure of 5.5×10^{-3} Torr, both magnitudes change their behavior due to better electron confinement enhanced by electron collisions with the background gas.

Figure 6 shows the dependence of the difference between the plasma potential and the first grid voltage on

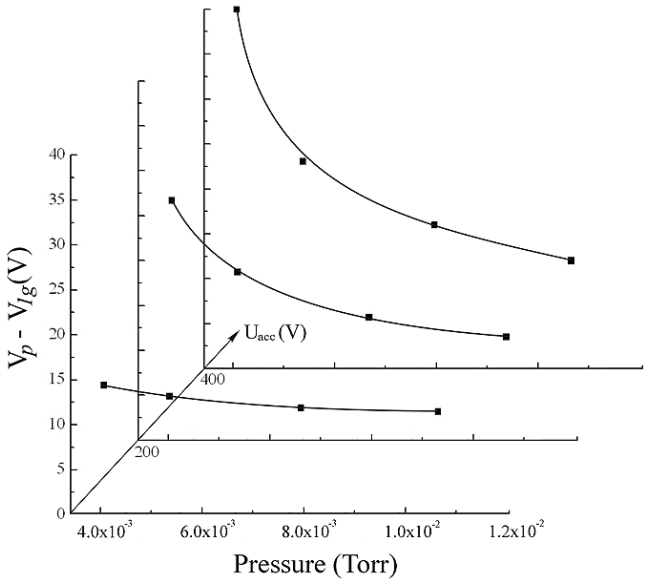

Fig. 6. $V_p - V_{1g}$ as a function of pressure and accelerating voltage.

the pressure and the accelerating voltage of the ICP ion source. $V_p - V_{1g}$ varied from 11.5 to 40 eV, reaching its maximum at lower pressures and higher accelerating voltages. Although, as was measured in Ref. 21, V_p can slightly differ from the mean ion energy within the range of $3 - 4$ eV, assuming the scale, we can consider these magnitudes equal.

IV. CONCLUSION

The effect of a beam energy increase compared to the preset value was studied by analyzing the IEDF obtained in the transition pressure range from 1×10^{-3} to 1×10^{-2} Torr and for high accelerating voltages on the electrode adjacent to the plasma. The plasma potential variation with pressure near the floating electrode was found not to exceed $3 - 5$ V, however, this magnitude increased up to 50 V when 400 V was applied to the first electrode. We believe that the main reasons for the plasma potential increase near the holes of the biased grid are sheath modification due to collisions and plasma boundary movement according to the continuity law that changes the charge balance in the sheath when the grid surface is comparable to the discharge volume.

Two slopes were found for the dependence of the current on the pressure, indicating mechanisms of ion extraction with and without collisions. The ion current inside the source linearly grew as the pressure increased; however, at the outlet of the ion optical system, this growth was not observed, which was caused by a plasma potential decrease and an ensuing beam defocusing near the grid holes. The described sequence of measurements can be taken as a basic conception for precise ion energy determination for the beams obtained with ICP sources, which is the main precursor to their application in nanotechnology.

ACKNOWLEDGMENTS

This work was supported by the National Program for Tera-level Nanodevices of the Korea Ministry of Science and Technology as one of the 21st Century Frontier Programs.

REFERENCES

[1] W. Hittorf, Ann. Phys. Chem. **21**, 90 (1984).
[2] M. Tuszewski and J. A. Tobin, J. Vac. Sci. Technol. A **14**, 1096 (1996).
[3] D. He, X. Wang, Q. Chen and J. Li, J. Korean Phys. Soc. **46**, S88 (2005).
[4] J. H. Park, N. E. Lee, Jaichan Lee, J. S. Park and H. D. Park, J. Korean Phys. Soc. **47**, S422 (2005).
[5] J. W. Lee, C. R. Abernathy, S. J. Pearton, C. Constantine, R. J. Shul and W. S. Hobson, Plasma Sources Sci. Technol. **6**, 499 (1997).
[6] M. A. Lieberman and A. J. Lichtenberg, *Principles of Plasma Discharges and Materials Processing* (Wiley, New York, 1994).
[7] J. R. Woodworth, M. E. Riley, P. A. Miller, G. A. Hebner and T. W. Hamilton, J. Appl. Phys. **81**, 5950 (1997).
[8] S. Humphries, J. Comp. Phys. **204**, 587 (2005).
[9] K. Okada, S. Komatsu and S. Matsumoto, J. Mater. Res. **14**, 578 (1999).
[10] M. J. Chung, D. H. Lee and G. Y. Yeom, Surface and Coatings Technology **171**, 231 (2003).
[11] B. A. Helmer and D. B. Graves, J. Vac. Sci. Technol. A **16**, 3502 (1998).
[12] T. Yunogami, K. Yokogawa and T. Mizutani, J. Vac. Sci. Technol. A **13**, 952 (1995).
[13] N. Hershkowitz, M.-H. Cho and J. Pruski, Plasma Sources Sci. Technol. **1**, 87 (1992).
[14] U. Kortshagen and M. Zethoff, Plasma Sources Sci. Technol. **4**, 541 (1995).
[15] J. Hopwood, Appl. Phys. Lett. **62**, 940 (1993).
[16] K. Okada, S. Komatsu and S. Matsumoto, J. Vac. Sci. Technol. A **21**, 1988 (2003).
[17] Y. Itikawa, M. Hayashi, A. Ichimura, K. Onda, K. Sakimoto, K.Takayanagi, M. Nakamura, H. Nishimura and T. Takayanagi, J. Phys. Chem. Ref. Data **15**, 985 (1986).
[18] K. Okada, S. Komatsu and S. Matsumoto, J. Vac. Sci. Technol. **17**, 721 (1999).
[19] J. S. Kim, M. V. Rao1, M. A. Cappelli, S. P. Sharma1 and M. Meyyappan, Plasma Sources Sci. Technol. **10**, 191 (2001).
[20] A. M. Budjanski, Ph.D. thesis, Kuibishev, 1989.
[21] J. S. Kim, M. V. Rao, M. A. Cappelli, S. P. Sharmal and M. Meyyappan, Plasma Sources Sci. Technol. **10**, 191 (2001).